J Geod (2011) 85:505–517
DOI 10.1007/s00190-011-0450-6

ORIGINAL ARTICLE

An evaluation of solar radiation pressure strategies for the GPS constellation

Ant Sibthorpe · Willy Bertiger · Shailen D. Desai · Bruce Haines · Nate Harvey · Jan P. Weiss

Received: 9 July 2010 / Accepted: 2 February 2011 / Published online: 19 February 2011

Abstract The subtle effects of different Global Positioning System (GPS) satellite force models are becoming apparent now that mature processing strategies are reaching new levels of accuracy and precision. For this paper, we tested several approaches to solar radiation pressure (SRP) modeling that are commonly used by International GNSS Service (IGS) analysis centers. These include the GPS Solar Pressure Model (GSPM; Bar-Sever and Kuang in The Interplanetary Network Progress Report 42-160, 2005) and variants of the so-called DYB model (Springer et al. in Adv Space Res 23:673–676, 1999). Our results show that currently observed differences between GPS orbit solutions from the various IGS analysis centers are in large part explained by differences between their respective approaches to modeling SRP. DYB-based strategies typically generate orbit solutions that have the smallest differences with respect to the IGS final combined solution, largely because the DYB approach is most commonly used by the contributing analysis centers. However, various internal and external metrics, including ambiguity resolution statistics and satellite laser ranging observations, support continued use of the GSPM-based approach for precise orbit determination of the GPS constellation, at least when using the GIPSY-OASIS software.

Keywords Solar radiation pressure (SRP) · Satellite orbits · IGS · Final combination · GPS

A. Sibthorpe (✉) · W. Bertiger · S. D. Desai · B. Haines · N. Harvey · J. P. Weiss
Jet Propulsion Laboratory, California Institute of Technology, Pasadena, CA, USA
e-mail: anthony.j.sibthorpe@jpl.nasa.gov

1 Introduction

Significant improvements in the accuracy of precise orbit determination solutions for the Global Positioning System (GPS) constellation of satellites have been realized over the last few years. The use of antenna calibrations (Hurst and Bar-Sever 1998; Mader 1999; Schmid et al. 2005) for both the transmitting satellites and the terrestrial receivers has been especially beneficial. Improved accuracy now makes it possible to analyze some of the smaller error sources for our orbital solutions. In this paper, we assess the relative performance of four approaches to modeling solar radiation pressure (SRP) on the GPS satellites, focusing on those most commonly adopted by International GNSS Service (IGS) analysis centers. Three are pure estimation strategies based upon variations of the so-called DYB model (Beutler et al. 1994; Springer et al. 1999a,b), while the fourth solves for small deviations from the GPS Solar Pressure Model (GSPM; Bar-Sever and Kuang 2004, 2005).

The three DYB approaches that we assess are based on our interpretation of the estimation strategy summaries provided by IGS analysis centers.[1] They estimate constant accelerations along a direct line from the spacecraft to the Sun (D), the spacecraft Y-axis around which the solar panels rotate (Y) and a third axis (B) chosen to complete a right-handed set of axes (see Fig. 1). In addition, once-per-orbital-revolution sine and cosine terms are estimated to accommodate unmodeled accelerations in the B direction. These periodic terms are a function of the orbit angle (u), measured between the projected Earth–Sun line and the position of the GPS satellite in the orbit plane. Of the three axes chosen, only the Y-axis can be defined as a constant in relation to the spacecraft geometry, while the D-axis 'tracks' the Sun and the

[1] ftp://igscb.jpl.nasa.gov/igscb/center/analysis/.

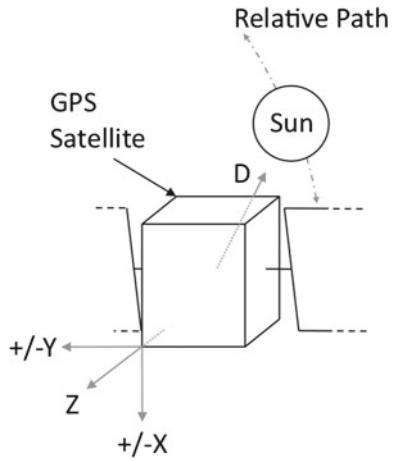

Fig. 1 DYB and XYZ satellite coordinate systems; the B axis is normal to the DY plane, and can be computed from the cross-product of D and Y

B-axis completes the right-handed set. The IGS summaries indicate that the majority of analysis centers, using a DYB-based approach during the year of our analysis period (2008), tended to use either no a priori SRP model or an a priori SRP model developed by the Center for Orbit Determination in Europe (CODE; Beutler et al. 1994). Recent work (Urschl et al. 2007) suggests that with a DYB-based approach, there is little difference between using the CODE a priori SRP model or no a priori SRP model; therefore, we do not use one here. In this paper, we consider three DYB-based strategies:

(a) DYBn = nominal, baseline approach as described above. Although no IGS analysis centers explicitly use this strategy, it provides a useful benchmark for the next two DYB approaches, which are variants of it.
(b) DYBa = DYBn with additional constant and periodic once-per-orbit-revolution accelerations estimated along-track (all constrained to ± 0.1 nm/s^2, 1-sigma).
(c) DYBi = DYBn with 'pseudo-stochastic' impulses (Beutler et al. 1994), sudden small constrained changes in velocity estimated at noon UTC (the center of each arc) for each satellite. We achieve this by estimating a small motor burn, or delta-V each day, constrained to 100 N (1-sigma).

In practice, the GSPM approach that we evaluate uses the GSPM model (Bar-Sever and Kuang 2004, 2005) as an a priori and estimates other parameters. This approach is being used operationally at the Jet Propulsion Laboratory's (JPL's) IGS analysis center. We note that our GSPM results might be biased in favor of this approach, as it was developed using GIPSY-OASIS. However, the US Air Force's GPS Master Control Station and Operational Control System have transitioned to GSPM, and use it very successfully in an operational context with completely independent software to compute the broadcast ephemerides uploaded to the GPS satellites (Creel et al. 2006). The GSPM a priori model, estimated from several years of flight data and composed of block-specific models, will not be perfectly correct for any given satellite on any given day. Therefore, in addition to this a priori model, we estimate a constant Y-axis bias (Fliegel and Gallini 1992) and a constant scale along the satellite to Sun direction, as well as small time-varying (stochastic) variations in model scale along the body-fixed spacecraft Z- and X-axes, and small stochastic changes along the Y-axis. Our methodology can be regarded as a "reduced-dynamic" approach (Wu et al. 1991), see Table 1 for details of key stochastic parameter values. For block IIA satellites, the Z-axis points to the geocenter, the Y-axis points along the solar panel rotation axis, and the X-axis resides in the same half-space as the Sun and completes a right-handed set of axes (see Fig. 1). For block IIR satellites, Z is the same as for the block IIA satellites, but X and Y are rotated by 180° (Bar-Sever and Kuang 2004). For eclipsing satellites, both our DYB and GSPM approaches set solar radiation forces to zero in the umbra, while a shadow factor is applied for penumbral transitions. Note that although the shadow factor is applied to the constant Y-axis bias, it is not used to scale stochastic changes along the Y-axis. In addition, GSPM provides a set of different block-specific a priori models for eclipsing satellites (Bar-Sever and Kuang 2005).

Table 1 Key stochastic parameter details

Parameter	Sigma (process noise)		Time	
	A priori	Steady state	Update (s)	Correlation (s)
Solar scale	1.00%	1.00%	3,611	14,400
Y bias	0.01 nm/s^2	0.01 nm/s^2	3,611	14,400

Solar scale values are valid for both X and Z parameters

Using JPL's GIPSY-OASIS software, we process data spanning all of 2008 (GPS weeks 1460-2 to 1512-3) to produce orbit solutions for the GPS constellation based on these DYB and GSPM SRP models/estimation strategies. We evaluate the resulting solutions based on a number of internal and external metrics:

1. day-to-day orbit overlaps;
2. day-to-day clock overlaps;
3. distribution of double difference carrier phase ambiguities;
4. satellite laser ranging (SLR) residuals;
5. day-to-day orbit differences versus IGS final orbits.

We present results of these tests below. We also apply metrics to the results of positioning terrestrial and low Earth orbiter receivers from our GPS orbit and clock solutions:

6. static receiver point-positioning repeatability;
7. GRACE A/B point-positioning cross-check with K-band ranges.

However, these positioning results are dominated by other errors sources, so we provide only a limited discussion of these metrics.

Additionally, we assess the translation of the terrestrial reference frame's Z-axis and compare Earth orientation parameters with values provided by the International Earth Rotation and Reference Systems Service (IERS).

2 Orbit determination approach

For this investigation, we followed the orbit determination approach adopted operationally at JPL, with identical input data, and changed only the SRP force modeling strategy to assess the relative accuracy and consistency of the resulting solutions. Measurement data are retrieved for a network of ground stations and a span of 30 h centered at noon on a given day, rather than the 24-h span commonly used by other IGS analysis centers. Stations are first vetted based on a number of data quality metrics (e.g. detected phase breaks), and 80 of the remaining sites are then selected to provide as evenly spaced a global distribution as possible. On any given day, the station and satellite selection is identical for each of the DYB and GSPM models. We use an elevation angle cutoff of 7°, IGS standard ground and satellite antenna calibrations, the global pressure and temperature (GPT) nominal troposphere model (Boehm et al. 2007), the tropospheric global mapping function (GMF) model (Boehm et al. 2006), IERS2003 standards (McCarthy and Petit 2004), FES2004 ocean loading and tidal gravity models (Lyard et al. 2006), and a GRACE-based (GGM02C) static gravity model (Tapley et al. 2005). Orbit solutions are transformed into the IGS05 frame—the IGS realization of the ITRF2005 reference frame (Altamimi et al. 2007; Ferland and Piraszewski 2009). Operationally, any solutions that produce undesirably large post-fit residuals for particular stations are re-run with those stations excluded. Here, however, for simplicity of processing, we just removed such days (about 15) from all solutions during the 1-year period.

3 Orbit overlaps

Each of our daily orbit solutions, centered on noon, spans a 30-h arc; hence, any two consecutive days overlap by 6 h. Differencing orbit solutions during these overlapping periods provides a direct check on daily orbit repeatability and consistency. To mitigate edge effects, we consider only the middle 5 h of each 6-h overlap, differencing positions given at 15-min intervals. There is a small possibility that these overlap results are biased in favor of our GSPM strategy due to the increased number of estimated stochastic parameters. Any such bias is, however, likely to be limited since the stochastic parameters are tightly constrained (see Table 1).

Figures 2 and 3 show 1D root mean square (RMS) values of orbit overlap differences, defined as 3D RMS of differences scaled down by a constant factor (see Eq. 1):

Maximum 1D RMS: 1D RMS of orbit differences for those GPS satellites with the largest day-to-day overlap orbit differences.
Median 1D RMS: Median (across available satellites in the solutions) 1D RMS of day-to-day overlap orbit difference.

$$1\mathrm{D} = 3\mathrm{D}\frac{1}{\sqrt{3}} \tag{1}$$

Our GSPM orbital solutions produce smaller average day-to-day orbit overlap differences, with less scatter, than do any of our DYB approaches. Note also that the DYBn strategy results in the least favorable orbit overlap

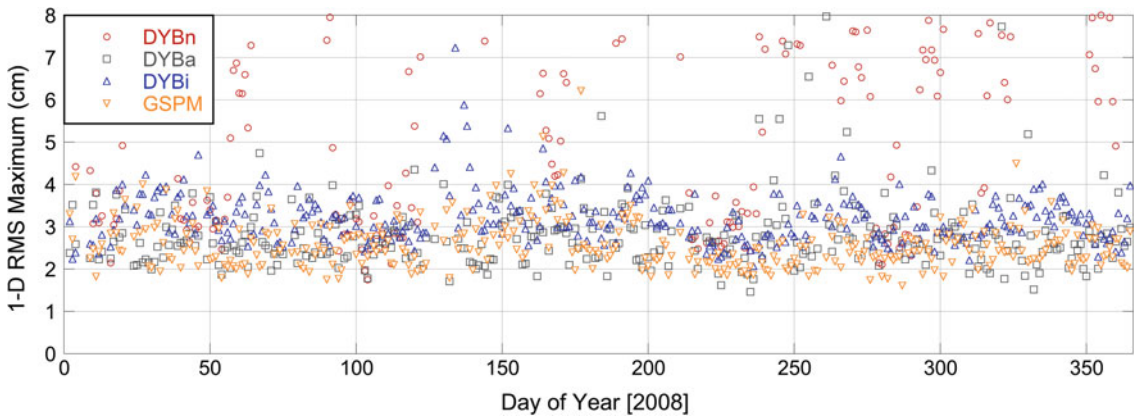

Fig. 2 Maximum 1D RMS orbit overlaps. Mean, 1-sigma (cm): DYBn (9.4, 6.5), DYBa (2.9, 2.0), DYBi (3.3, 1.5), GSPM (2.6, 0.6)

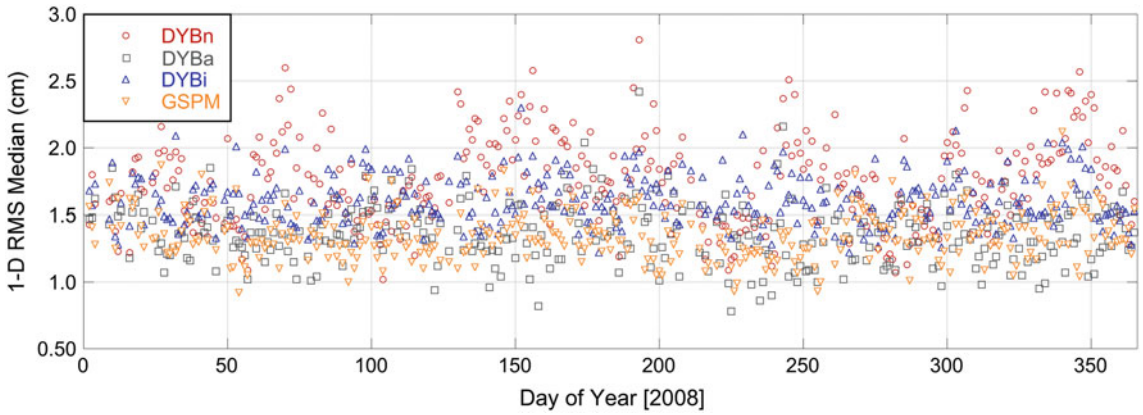

Fig. 3 Median 1D RMS orbit overlaps. Mean, 1-sigma (cm): DYBn (1.8, 0.3), DYBa (1.4, 0.2), DYBi (1.6, 0.2), GSPM (1.3, 0.2)

repeatability, with most of its results actually beyond the scale of Fig. 2.

4 Clock overlaps

As with the orbit solutions, there is a 6-h overlap between satellite clock estimates from consecutive daily solutions, and again we consider differences from only the central 5 h of overlapping estimates. To minimize the offset effects of using different GPS pseudorange data and having possibly chosen different reference clocks on adjacent days, a linear fit to clock differences for the entire GPS constellation is first removed. For each SRP strategy, we compute daily RMS of overlapping clock differences taken at 15-min intervals for each GPS satellite. Figures 4 and 5 show the maximum and RMS (across all available satellites) scatter of adjusted clock differences in each day-to-day overlap for each approach. The DYBa approach results in smaller mean overlap values, although with slightly larger scatter than some of the other approaches. Both DYBi and DYBn produce less favorable results than GSPM.

5 Ambiguity resolution

Our approach uses the Kalman filter/smoother in GIPSY-OASIS to estimate a variety of parameters, including real-valued phase biases. Double difference phase bias ambiguities (Blewitt 1989) are then resolved for a more accurate solution. We assume that:

1. A tighter distribution of phase bias narrow-lane double differences around integers indicates better unresolved phase bias estimates.
2. More accurate unresolved phase bias estimates yield more accurate unresolved position and clock estimates.
3. A more accurate unresolved solution leads to a more accurate resolved solution.

In our experience, independent cross-checks have shown that when we produce better position and clock estimates, double differenced narrow-lane ambiguities (Blewitt 1989) usually cluster more tightly around integers. Rather than

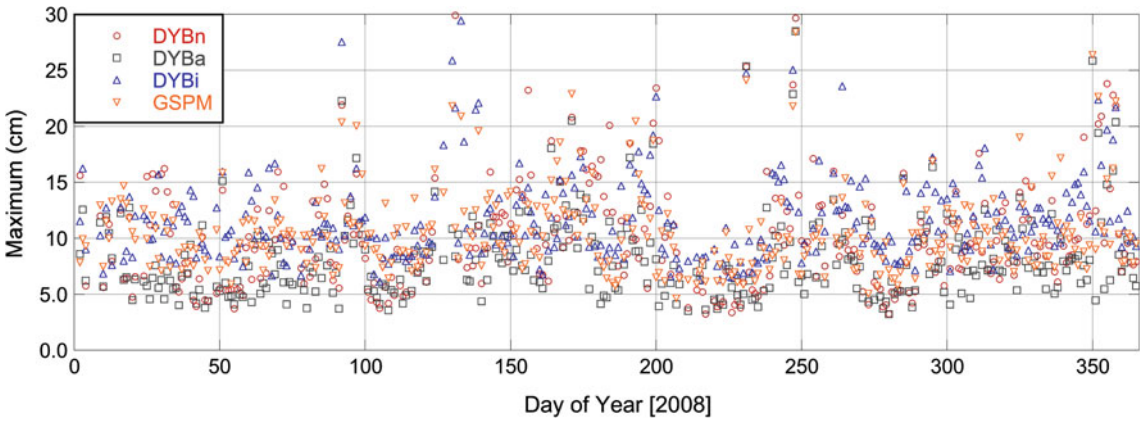

Fig. 4 Maximum clock overlaps. Mean, 1-sigma (cm): DYBn (10.7, 6.6), DYBa (8.5, 5.0), DYBi (11.8, 4.4), GSPM (10.6, 4.0)

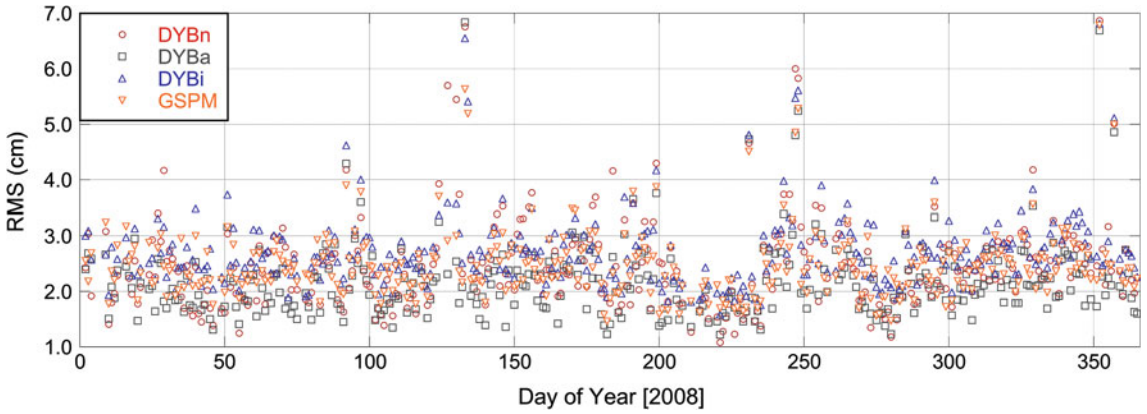

Fig. 5 RMS clock overlaps. Mean, 1-sigma (cm): DYBn (2.5, 1.1), DYBa (2.3, 1.0), DYBi (2.8, 0.9), GSPM (2.5, 0.9)

rely on standard deviation around the nearest integer, a statistic dominated by outliers and badly determined double differences, we chose a more robust statistic to assess clustering: proportion of narrow-lane double differences within a "reasonable distance" of the nearest integer. We chose 0.10 cycles as a "reasonable distance" because our current operational ambiguity resolution settings do not resolve double-differenced narrow-lanes beyond this threshold. To avoid obvious problem cases, we only considered narrow-lanes of double differences for which:

1. All four phase bias arcs overlapped by at least 1 h.
2. We resolved the double differenced wide-lane with high confidence.

Figure 6 shows the percentage of narrow-lane double differences more than 0.1 cycles from the closest integer for each SRP model. The GSPM solutions consistently produce a substantially higher proportion of narrow-lane double differences closer to integers than DYBn, DYBa or DYBi. It is worth noting that this is an independent assessment, since none of the SRP strategies presented here were tuned to this metric.

Figure 7 shows the standard deviations of these percentage values after they have been binned according to the number of satellites in eclipse. All DYB approaches show greater dependence on the number of satellites in eclipse than GSPM, suggesting an explanation for the more periodic behavior of the DYB approaches seen in Fig. 6.

6 SLR

JPL's SLR analysis software has been recently updated to include additional offset (shim) corrections for the center-of-mass positions of the retro-reflectors on SVN35 (+11 mm) and SVN36 (+13 mm) (Davis and Trask 2007), and a relatively new model and mapping function for tropospheric delay at optical wavelengths (Mendes et al. 2002; Mendes and Pavlis 2004). All orbits were processed using identical SLR strategies and only points common to all solutions

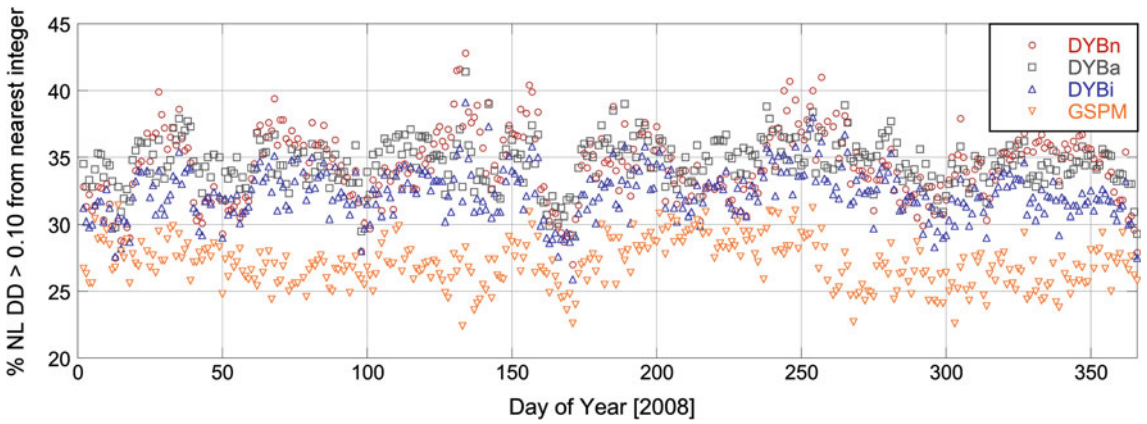

Fig. 6 Percentage of all narrow-lane double differences further than 0.1 cycles from nearest integer. Mean, 1-sigma (%): DYBn (34.3, 2.7), DYBa (34.6, 1.8), DYBi (32.3, 1.9), GSPM (27.1, 1.7)

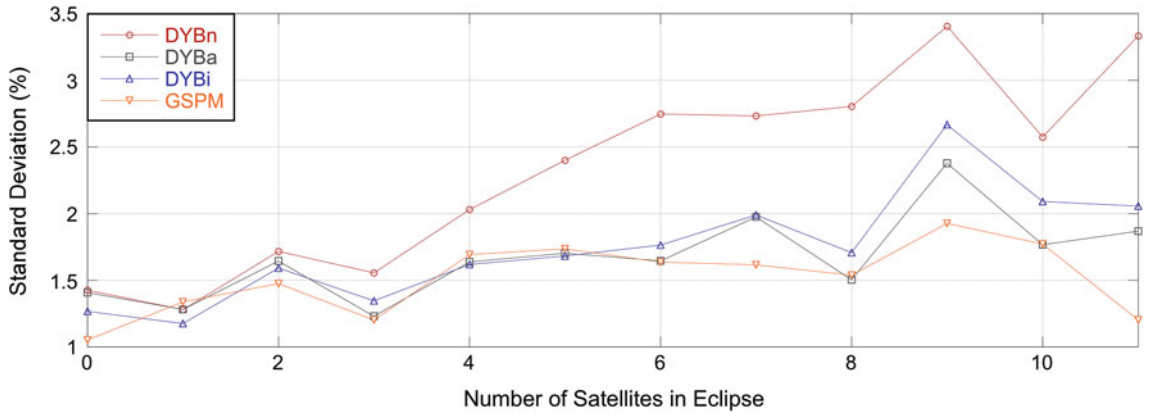

Fig. 7 Scatter of percentage narrow-lane double differences further than 0.1 cycles from nearest integer according to the number of satellites in eclipse

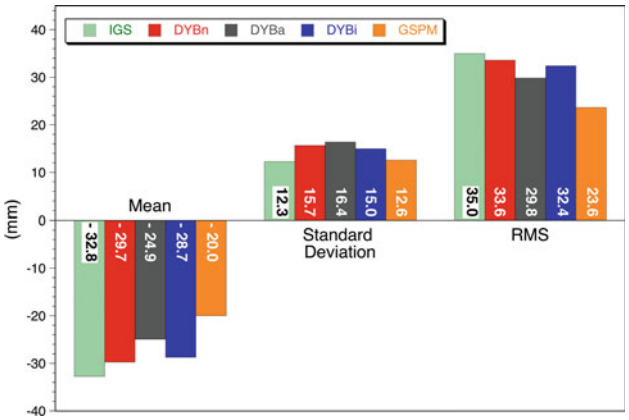

Fig. 8 SLR residuals to SVN35 (1,281 observations)

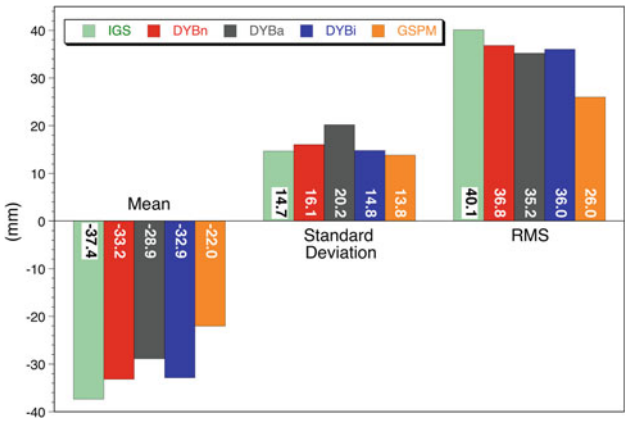

Fig. 9 SLR residuals to SVN36 (2,145 observations)

are included in the results. Operational GIPSY-OASIS orbit processing is configured to delete satellites based on NANU[2] information. NANUs for SVN35 caused this satellite to be deleted for about 9 weeks during August and September 2008. Due to this complication, our IGS final combined orbit solution SLR results for SVN35 (Fig. 8) and SVN36 (Fig. 9) have been computed separately, using only those days where SVN35 and 36 are also present in our solutions. Figures 8 and 9 show results for our different SRP orbit solutions and also for the IGS final combined solution. It is clear from these figures that GSPM has the advantage in terms of both mean and scatter over all the DYB solutions. The IGS final orbits have the highest mean values, with standard deviations comparable to GSPM.

We also make use of a plot style developed by Flohrer (2008) to display our SLR residuals, as it allows easier interpretation of the behavior during different eclipse regimes. The beta angle (β) is the acute angle between the line from the center of the Earth to the Sun and the Earth–Sun line projected onto the GPS satellite orbit plane, and can be thought of as the solar elevation angle. The orbit angle (u), defined above, can be thought of as the solar azimuth angle. Two charts are presented for each SRP strategy (see Fig. 10). In the upper plot, SLR residuals are shown as a function of both β and u. At and near to a value of $u = 0°$ the satellites are at orbit noon, while at and near a value of $u = 180°$ the satellites are at orbit midnight (Bar-Sever 1996). At absolute β values less than about 14°, the satellites are in eclipse season. The lower plot shows a profile of the SLR residuals solely as a function of u, together with a moving average using a window size of 100 points. As we have less tracking data for SVN35, we only show plots for SVN36. The most obvious differences in Fig. 10 are for GSPM, which has smaller residuals in the center of its upper plot, a region representative of satellites in eclipse. Both DYBi and GSPM offer smaller residuals in the area from $u = 0$ to $u = 90°$. Bearing in mind that all models use the same yaw attitude algorithm, the results overall suggest that the GSPM approach provides

[2] http://www.navcen.uscg.gov/gps/nanu.htm.

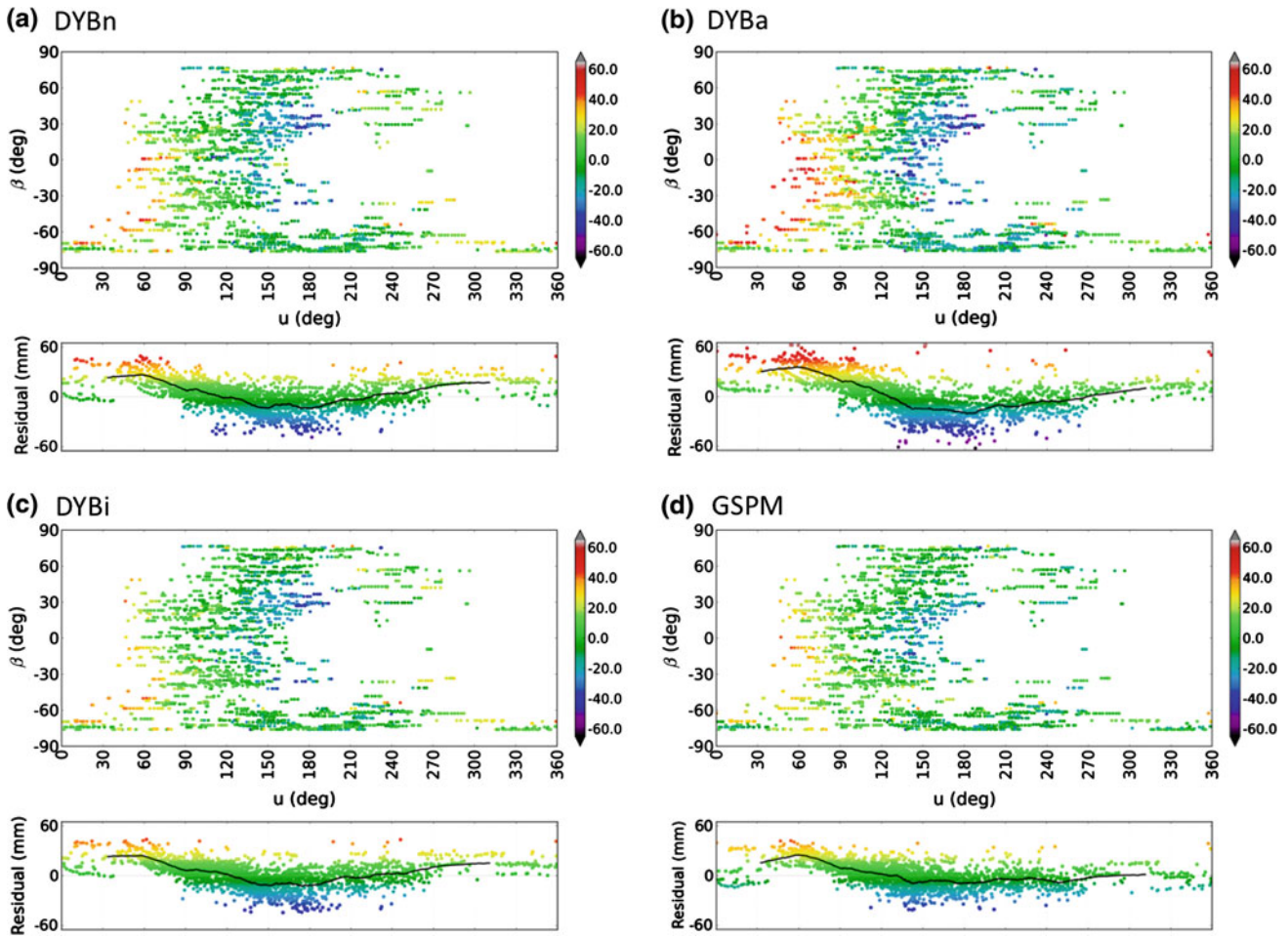

Fig. 10 One-way SLR residuals in millimeters for each strategy (SVN36): *upper plots* show residuals plotted against β and u after removing an average bias; *lower plots* show the same values against u only, including a moving average with a window size of 100 points (*solid black line*). Standard deviation of moving average (mm): DYBn (10.7), DYBa (16.0), DYBi (9.5), GSPM (8.9)

better SRP modeling for eclipsing satellites during 2008 than any of the DYB-based approaches, perhaps due largely to its use of different block-specific a priori models for eclipsing satellites. GSPM also has a flatter moving average curve in the lower plot, and fewer measurements with high (dark red or blue) residuals.

7 Orbit differences versus IGS

The IGS is responsible for the coordination, analysis, product generation and dissemination of data from more than 350 permanent Global Navigation Satellite System (GNSS) receivers worldwide. During 2008, eight core analysis centers (ACs) were responsible for contributing individual GPS orbit solutions to the IGS analysis center coordinator who combines them into a single IGS final combined orbit product. The idea behind this approach is that as "[t]he AC's use a variety of independently developed software packages, different estimation strategies and different sets of stations" (Dow et al. 2005), a solution incorporating output from each AC should be the most robust.

In this section, we compare our DYB- and GSPM-based orbital solutions to the IGS final products. To account for frame differences, we computed and applied a six-parameter transformation for each of our daily orbit solutions to minimize the RMS of orbit differences from the IGS combined solution. On each day, for each of our SRP strategies, we computed the RMS of orbit differences over all GPS satellites, and we present **Minimum 1D RMS**: 1D RMS of orbit differences for the transformed GPS constellation whose solution matches the IGS final product most closely.

Figure 11 plots the minimum 1D RMS for each daily orbit solution. Although our DYBn approach fares worst in this test, our DYBa and DYBi solutions match IGS final products substantially more closely than do our GSPM solutions, especially after the obvious step change on November 23, 2008

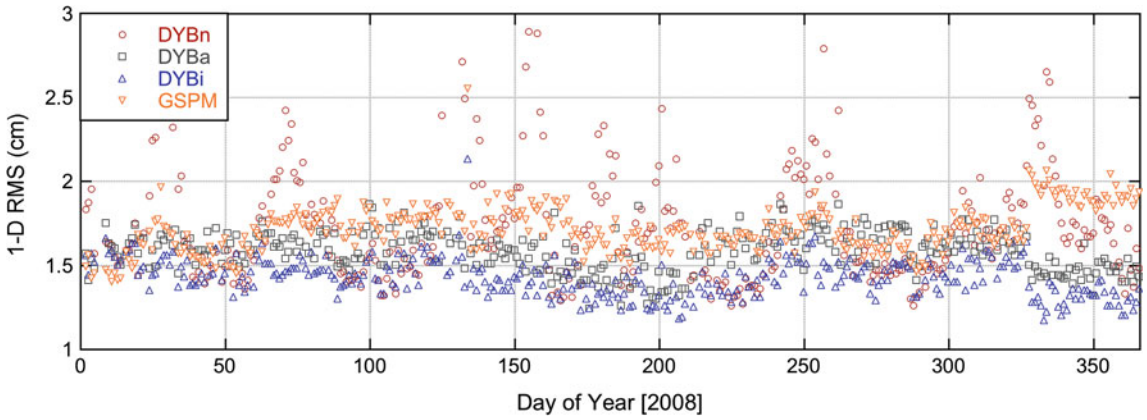

Fig. 11 Minimum 1D RMS orbit differences with respect to the IGS final combined solution. Mean, 1-sigma (cm): DYBn (1.8, 0.4), DYBa (1.6, 0.4), DYBi (1.4, 0.1), GSPM (1.7, 0.1)

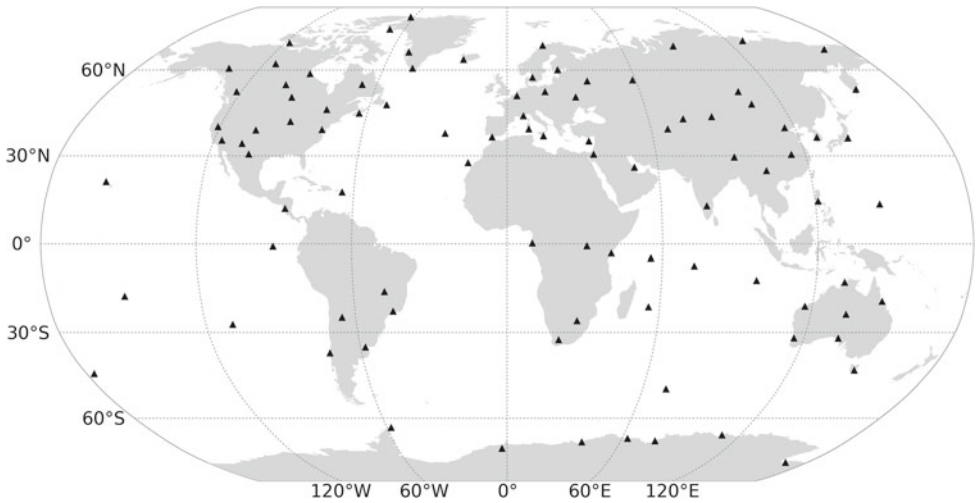

Fig. 12 IGS05 sites used for PPP station repeatability tests

(day of year 328). On day 328, the GeoForschungsZentrum (GFZ) IGS analysis center changed their SRP model from a unique combination of 'GSPM + noon impulse', to a close relative of DYBi (Gerd Gendt, pers comm). During and after 2008, between five and six of the eight IGS core analysis centers were using a DYB formulation to account for the effects of SRP, of which one to two were not using an a priori radiation pressure model. Results below are closely matched with operational results for final GPS orbits as reported by the IGS analysis center coordinator.[3]

8 Station repeatability

For each day of 2008, we conducted precise point positioning (PPP) (Zumberge et al. 1997) without integer phase ambiguity resolution using fixed GPS orbits and clocks from each SRP strategy for 106 IGS05 frame definition sites. After 3-sigma filtering per station, we calculated position repeatabilities in east, north and up (ENU) relative to the IGS05 station positions (Ferland and Piraszewski 2009) at epoch. Points filtered from any one strategy were eliminated from all strategies before further processing. Per station standard deviations in ENU were then calculated for any station having a minimum of 30 days of PPP results. This processing chain left us with 94 stations, as shown in Fig. 12.

We report median standard deviations of station repeatability in Fig. 13. Differences between each strategy are admittedly small (0.1–0.2 mm), but they are consistent; with DYBa showing the worst repeatabilities in all three directions, DYBn and DYBi are identical at the tenth of a millimeter level, while GSPM shows marginally better repeatabilities in all three directions.

This metric is not completely independent of the orbit solutions. The set of 80 stations used to generate the orbit solutions, a subset of which is aligned (fiducialized) to the

[3] http://acc.igs.org/.

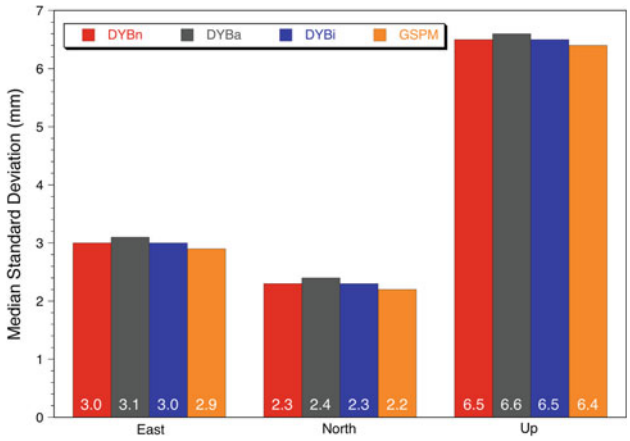

Fig. 13 Station repeatability—median standard deviation in ENU (mm)

IGS05 reference frame, changes daily and, over a year it is uncommon to find a station not included in the daily orbit solutions at least once. On average, for any given day, 55% of the stations included in the PPP analysis were also used to estimate the orbit. However, Bertiger et al. (2010) report very similar station repeatability values for 6 months of JPL's operational orbits, suggesting that biases resulting from any such inter-dependence are mitigated by long-period averaging.

9 GRACE K-band comparison

The GRACE tandem mission (Tapley et al. 2004) consists of two satellites flying in near identical orbits at an altitude of just under 500 km. The inter-satellite distance, maintained at between 170 and 220 km, is measured at the micron level by K-band ranging systems onboard each satellite. The GRACE satellites also carry advanced dual-frequency "BlackJack" GPS receivers for precise orbit determination. Comparing K-band ranging (KBR) measurements to independent GPS-based orbit solutions for the GRACE satellites—determined from data referenced to each of our GPS orbit solutions—allows us to independently assess the accuracy of our orbit solutions for the GPS constellation. Because the sensitivity of this test was uncertain, we only compared solutions for DYBi, the model most closely representing that used by most IGS analysis centers, and GSPM, across the first half of 2008. In Fig. 14, we show daily KBR-GPS standard deviations, with summary statistics given in Table 2. As with the station repeatability results, the differences are not only small, but also show marginally better performance from the orbit solutions that use the GSPM strategy.

10 Consistency and accuracy of the reference frame and earth orientation

10.1 Reference frame: non-fiducial to IGS05

Our orbit determination strategy begins with a fiducial-free approach, which simultaneously estimates station coordinates (1-m a priori sigma) and satellite positions. In a subsequent step, fiducial solutions are computed by aligning a sub-set of stations to their IGS05 positions. A seven-parameter Helmert transformation is used to describe the transformation between the station estimates from the non-fiducial solution with respect to the IGS05 reference frame. We focus on the recovered Z-axis translations (geocenter motion) as they are almost an order of magnitude larger than those along X or Y, and because Haines et al. (2004) showed that orbit centering along the Earth's Z-axis is significantly affected at the centimeter level by SRP model scale differences as small as 7%.

Figure 15 shows the difference between weekly averages of GPS-derived Z-axis translation components, required to fiducialize our free solutions, and independent weekly Z-axis translations derived from SLR measurements (Minkang Cheng, pers comm, see also Cheng et al. 2010), after carefully accounting for sign conventions. Strong agreement can be seen among all the DYB solutions, which collectively disagree with GSPM by up to 20–30 mm. The DYB solutions display a bias and a strong annual and/or possibly draconitic signal, while the GSPM solution has a larger bias and a smaller scatter. These results suggest that limiting error sources affect all strategies, and the annual amplitude for each is almost an order of magnitude larger than that expected from geocenter motion (Bouille et al. 2000; Moore and Wang 2003; Lavallee et al. 2006; Kang et al. 2009). Although a longer time series is outside the scope of this paper, the orbit centering issue and its relationship to SRP modeling certainly warrants further investigation.

10.2 EOPs: X/Y polar motion and length of day (LOD)

The IERS currently provides Earth orientation estimates with the highest available accuracy and precision, drawn from observations made by Very Long Baseline Interferometry (VLBI), SLR, GPS and Doppler Orbitography and Radiopositioning Integrated by Satellite (DORIS). We directly difference our estimates of X-pole, Y-pole and LOD with IERS Bulletin A (IAU2000) Earth orientation values, as these parameters are sensitive to systematic GPS orbit modeling errors (Lichten et al. 1992; Ray 1996; Gross 2009). In Figs. 16, 17 and 18, we show moving averages of all differences using a window size of 10 points to reduce visual clutter; statistics given in the figure captions always refer to

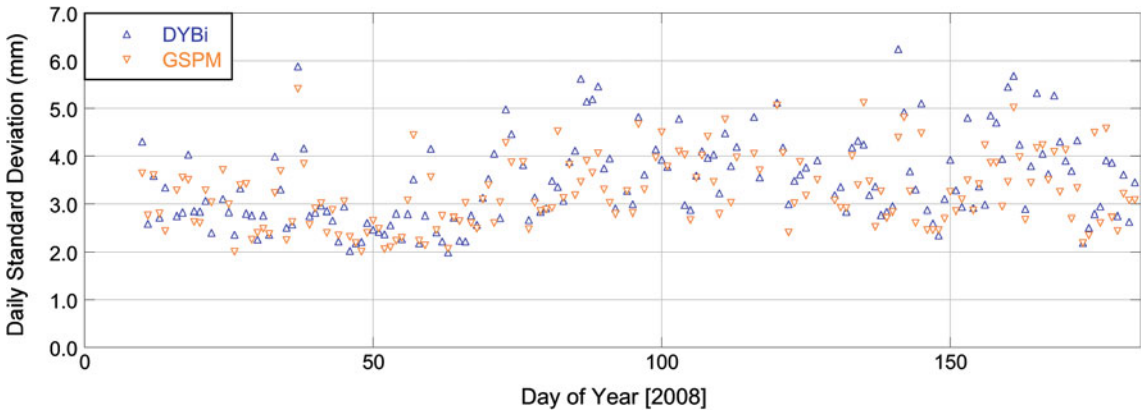

Fig. 14 Daily standard deviations of GRACE KBR–GPS ranges, following a 3-sigma edit

Table 2 Inter-satellite range differences between GPS orbit solutions

	Mean (mm)	Stdev (mm)	#obs
DYBi	3.4	0.9	160
GSPM	3.2	0.7	160

The GSPM standard deviations are smaller than the DYBi standard deviations for 63% of the observations retained (iterative 3-sigma edit applied, same points deleted from both solutions)

the raw data. For reference, 1 μs is equivalent to ∼31 μm when expressed as a distance at the surface of the Earth.

The GSPM approach yields a slightly reduced mean and a smaller scatter for X-pole. Apart from one or two excursions, DYBa, DYBi and GSPM display a very similar trend; DYBn is markedly different, though not necessarily worse. The amplitude of the differences between the IERS values and our X-pole estimates are at the level of a few millimeters, though in general results from individual SRP strategies differ from each other only at the level of a few tenths of a millimeter. The situation is very similar for Y-pole, although an annual signal is discernible for all strategies. For LOD, DYBn has the smallest mean and DYBi has the smallest scatter relative to the other solutions. It seems likely that values for GSPM have been unduly affected by the excursions around days of year 20 and 250, which are still under investigation.

The most conspicuous behavior comes from DYBa's LOD estimates, which contain a clear semi-annual signal, indicating that LOD estimation is problematic for DYBa. The effect is probably due, in large part, to the close relationship between the along-track component and the satellite orbital nodes; any nodal net rate of change directly affects LOD (Ray 1996). To test the sensitivity of LOD to the constraints we placed upon the along-track estimates, we ran an additional year of orbit solutions with essentially the same model as DYBa but without a priori constraints for the constant and periodic once-per-orbit-revolution along-track accelerations; we call this model DYBa_free. Although it might be

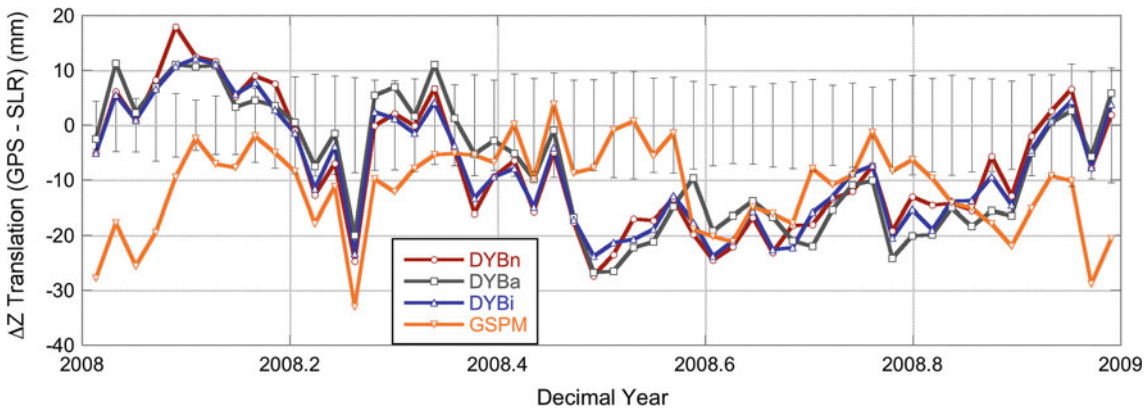

Fig. 15 Weekly delta Z translation components recovered from the transformation between free and fiducial (IGS05) solutions with respect to SLR. *Vertical error bars* are 1-sigma values for the SLR data. Mean, 1-sigma (mm): DYBn (−7.8, 11.3), DYBa (−7.3, 11.4), DYBi (−8.1, 10.5), GSPM (−11.4, 8.1)

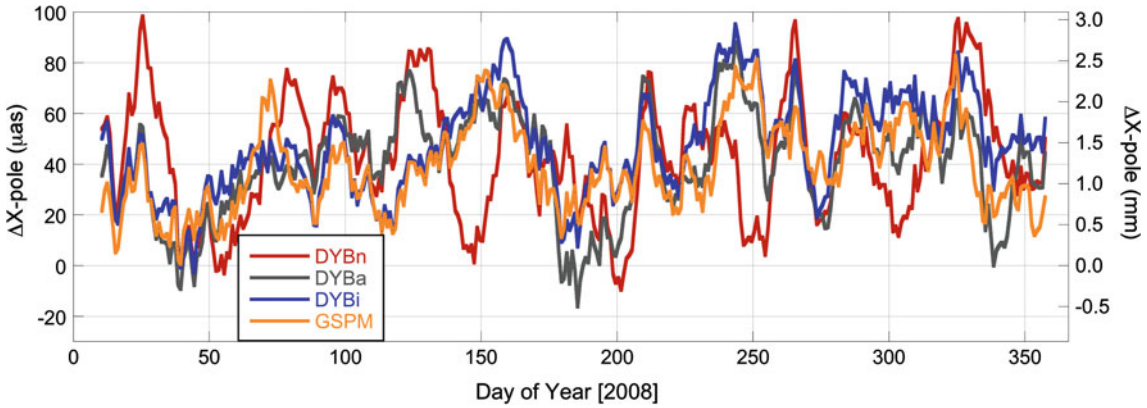

Fig. 16 Delta *X*-pole moving average with respect to IERS A, window size of 10 points. Mean, 1-sigma (μs): DYBn (42.9, 56.3), DYBa (41.3, 53.9), DYBi (47.5, 54.1), GSPM (37.9, 54.8)

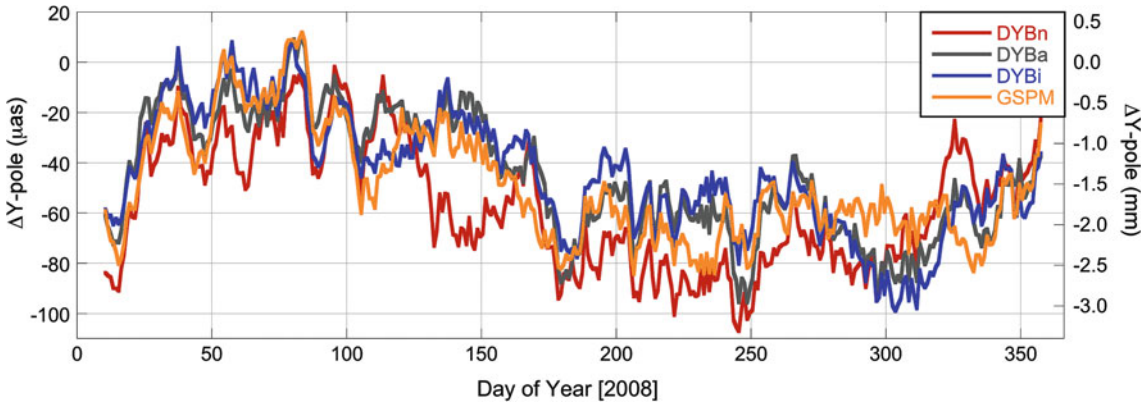

Fig. 17 Delta Y-Pole moving average with respect to IERS A, window size of 10 points. Mean, 1-sigma (μs): DYBn (−56.3, 54.0), DYBa (−44.9, 50.0), DYBi (−44.1, 49.4), GSPM (−47.8, 49.2)

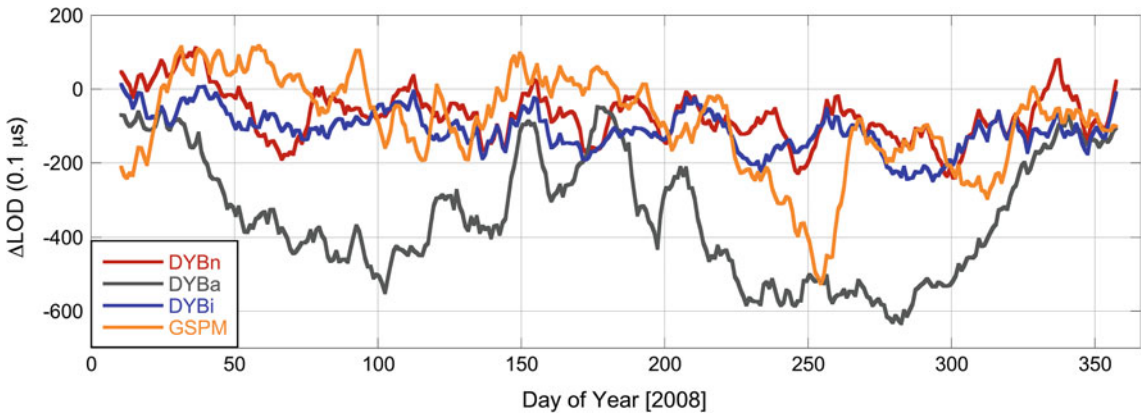

Fig. 18 Delta LOD moving average with respect to IERS A, window size of 10 points. Mean, 1-sigma (0.1 μs/d): DYBn (−69.1, 152.2), DYBa (−332.1, 228.8), DYBi (−109.6, 136.3), GSPM (−89.9, 206.3)

possible to further tune this along-track parameter, Fig. 19 demonstrates that the a priori sigma of the along-track acceleration is strongly linked with estimates of LOD. In fact, contamination of GPS LOD estimates by additional SRP parameters has been previously documented (Springer et al. 1999a).

11 Conclusions

In this paper, we tested four SRP parameterizations for the GPS constellation that are at present commonly adopted by most IGS analysis centers. The parameterizations included a stochastic GSPM-based approach (GSPM) and three

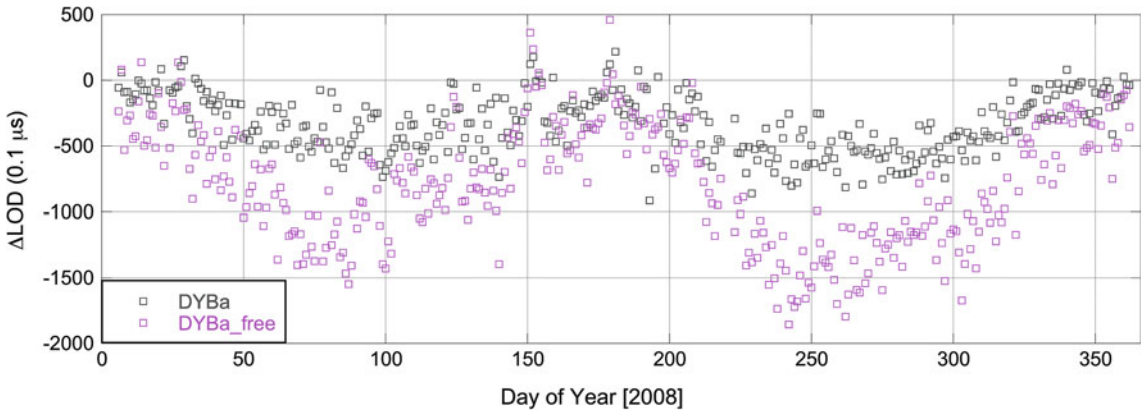

Fig. 19 Delta LOD for DYBa and DYBa_free. Mean, 1-sigma (0.1 μs/d): DYBa (−332.1, 228.8), DYBa_free (−787.9, 457.2)

dynamic DYB-based approaches (DYBn, DYBa and DYBi). JPL's IGS contributions currently use the GSPM approach, while most IGS analysis centers use a DYB-based strategy. We evaluated 1 year of precise orbit and clock solutions, generated using each of these strategies, with a range of internal and external quality metrics. Our results show that by adopting a DYB formulation we achieved much closer agreement between our GPS orbit solutions and IGS combined final products. However, the various metrics we present here suggest that doing so (at least within the GIPSY-OASIS software package) would not produce more accurate orbit solutions. A comparison of ambiguity resolution statistics strongly supports our GSPM-based approach. Taken together, orbit overlaps, SLR tracking residuals, station repeatabilities, and GRACE K-band ranging statistics also suggest that we produce more accurate solutions with our GSPM-based approach, while clock overlaps and LOD favor DYB-based approaches.

Our results show that solutions from most of the IGS analysis centers have achieved sufficient accuracy to uncover systematic differences due to SRP modeling strategies. A majority-voting scheme is used to generate the IGS combined products. As such, differences between products from individual analysis centers with respect to the IGS combined products systematically favor the DYB-based approaches used by most analysis centers. Accordingly, the smallest differences do not necessarily reflect the highest accuracy.

Our GSPM-based approach employs a different SRP parameterization as well as stochastic instead of dynamic parameter estimation. Based on several years of flight data, the a priori GSPM model has the benefit of representing, to some degree, the secular and higher frequency signals of radiation pressure effects on actual GPS satellites. Our tightly constrained stochastic parameter estimation is designed to complement this foundation by additionally determining low frequency errors in the SRP model. However, the relative contribution of the a priori GSPM model versus the tightly constrained stochastic parameter estimation to the improved orbit accuracy is unclear. As such, a hybrid approach that adopts the DYB strategy with stochastic parameter estimation merits future investigation.

Acknowledgments The research was carried out at the Jet Propulsion Laboratory (JPL), California Institute of Technology (© 2010 California Institute of Technology, government sponsorship acknowledged), under a contract with the National Aeronautics and Space Administration. Our thanks go to Gerd Gendt and Tim Springer for providing additional information about the solar radiation pressure modeling and estimation strategies used by GFZ and ESA, respectively. We are grateful to the IGS for making available their final combined orbit products (Dow et al. 2009), Minkang Cheng, Da Kuang, Yoaz Bar-Sever and the four anonymous reviewers who helped to improve this article.

References

Altamimi Z, Collilieux X, Legrand J, Garayt B, Boucher C (2007) ITRF2005: a new release of the international terrestrial reference frame based on time series of station positions and Earth orientation parameters. J Geophys Res 112(B09401). doi:10.1029/2007JB004949

Bar-Sever Y (1996) A new model for GPS yaw attitude. J Geodesy 70:714–723

Bar-Sever Y, Kuang D (2004) New empirically derived solar radiation pressure model for global positioning system satellites. The Interplanetary Network Progress Report 42-159. http://ipnpr.jpl.nasa.gov/progress_report/42-159/title.htm, accessed 04/15/2009

Bar-Sever Y, Kuang D (2005) New empirically derived solar radiation pressure model for global positioning system satellites during eclipse seasons. The Interplanetary Network Progress Report 42-160. http://ipnpr.jpl.nasa.gov/progress_report/42-160/title.htm, accessed 04/15/2009

Bertiger W, Desai SD, Haines B, Harvey N, Moore AW, Owen S, Weiss JP (2010) Single receiver phase ambiguity resolution with GPS data. J Geodesy (in press)

Beutler G, Brockmann E, Gurtner W, Hugentobler U, Mervart L, Rothacher M (1994) Extended orbit modeling techniques at the

CODE processing center of the International GPS Service for geodynamics (IGS): theory and initial results. Manuscr Geod 19: 367–386

Blewitt G (1989) Carrier phase ambiguity resolution for the global positioning system applied to geodetic baselines up to 2000 km. J Geophys Res 94(B8):10187–10203

Boehm J, Heinkelmann R, Schuh H (2007) Short note: a global model of pressure and temperature for geodetic applications. J Geodesy 81:679–683

Boehm J, Niell A, Tregoning P, Schuh H (2006) Global Mapping Function (GMF): a new empirical mapping function based on numerical weather model data. Geophys Res Lett 33:L07304. doi:10.1029/2005GL025546

Bouille F, Cazenave A, Lemoine JM, Cretaux JF (2000) Geo-centre motion from the DORIS space system and laser data to the LAGEOS satellites: comparison with surface loading data. Geophys J Int 143(1):71–82

Cheng MK, Ries JC, Tapley BD (2010) Geocenter variations from SLR, REFAG2010, France, October 7. Available at http://iag.ign.fr/abstract/refag2010_program.html

Creel T, Dorsey AJ, Mendicki PJ, Little J, Mach RG, Renfro BA (2006) New, improved GPS, GPS World. Available at http://www.gpsworld.com/gnss-system/gps-modernization/new-improved-gps-4014?page_id=1

Davis MA, Trask AJ (2007) Insight into the GPS navigation product accuracy using the SLR measurements. Available at http://ilrs.gsfc.nasa.gov/docs/davisgpstray.pdf

Dow JM, Neilan RE, Gendt G (2005) The International GPS Service: celebrating the 10th anniversary and looking to the next decade. Adv Space Res 36:320–326

Dow JM, Neilan RE, Rizos C (2009) The International GNSS Service in a changing landscape of Global Navigation Satellite Systems. J Geodesy 83: 191–198. doi:10.1007/s00190-008-0300-3

Ferland R, Piraszewski M (2009) The IGS-combined station coordinates, Earth rotation parameters and apparent geocenter. J Geodesy 83:385–392

Fliegel HF, Gallini TE (1992) Global positioning system radiation force model for geodetic applications. J Geophys Res 97(B1):559–568

Flohrer C (2008) Mutual validation of satellite-geodetic techniques and its impact on GNSS orbit modeling. PhD Thesis

Gross R (2009) Validating Earth orientation series with models of atmospheric & oceanic angular momenta. In: Proceedings of AGU Fall meeting, San Francisco, September 14–18

Haines B, Bar-Sever Y, Bertiger W, Desai SD, Willis P (2004) One-centimeter orbit determination for Jason-1: new GPS-based strategies. Marine Geodesy 27:299–318

Hurst KJ, Bar-Sever Y (1998) In-situ GPS antenna phase center calibration. OPS/MET, Tokyo, Japan

Kang Z, Tapley B, Chen J, Ries J, Bettadpur S (2009) Geocenter variations derived from GPS tracking of the GRACE satellites. J Geodesy 83:895–901

Lavallee DA, van Dam T, Blewitt G, Clarke PJ (2006) Geocenter motions from GPS: a unified observation model. J Geophys Res 111(B05405). doi:10.1029/2005JB003784

Lichten SM, Marcus SL, Dickey JO (1992) Sub-daily resolution of Earth rotation variations with global positioning system measurements. Geophys Res Lett 19(6):537–540

Lyard F, Lefèvre F, Letellier T, Francis O (2006) Modelling the global ocean tides: a modern insight from FES2004. Ocean Dyn 56:394–415

Mader G (1999) GPS antenna calibration at the national geodetic survey. GPS Solut 3(1):50–58

McCarthy DD, Petit G (2004) IERS conventions (2003). IERS Conventions Centre, Technical Note 32

Mendes VB, Pavlis EC (2004) High-accuracy zenith delay prediction at optical wavelengths. Geophys Res Lett 31:L14602. doi:10.1029/2004GL020308

Mendes VB, Prates G, Pavlis EC, Pavlis DE, Langley RB (2002) Improved mapping functions for atmospheric refraction correction in SLR. Geophys Res Lett 29:53-1–53-4

Moore P, Wang J (2003) Geocentre variation from laser tracking of LAGEOS 1/2 and loading data. Adv Space Res 31:1927–1933

Ray JR (1996) Measurements of length of day using the Global Positioning System. J Geophys Res 101(B9):20141–20149

Schmid R, Rothacher M, Thaller D, Steigenberger P (2005) Absolute phase center corrections of satellite and receiver antennas. GPS Solut 9(4): 283–293. doi:10.1007/s10291-005-0134-x

Springer TA, Beutler G, Rothacher M (1999) A new solar radiation pressure model for GPS. Adv Space Res 23:673–676

Springer TA, Beutler G, Rothacher M (1999) Improving the orbit estimates of the GPS satellites. J Geodesy 73(3):147–157

Tapley BD, Bettadpur S, Watkins S, Reigber C (2004) The gravity recovery and climate experiment: mission overview and early results. Geophys Res Lett 31(L09607). doi:10.1029/2004GL019920

Tapley B, Ries J, Bettadpur S, Chambers D, Cheng M, Condi F, Gunter B, Kang Z, Nagel P, Pastor R, Pekker T, Poole S, Wang F (2005) GGM02—an improved Earth gravity field model from GRACE. J Geodesy. doi:10.1007/s00190-005-0480-z

Urschl C, Beutler G, Gurtner W, Hugentobler U, Ostini L, Ploner M (2007) Assessing the quality of GNSS orbit models using SLR. European Geophysical Union, Vienna, Austria, April 16–20

Wu SC, Yunck TP, Thornton CL (1991) Reduced-dynamic technique for precise orbit determination of low Earth satellites. J Guid Control Dyn 14(1):24–30

Zumberge JF, Heflin MB, Jefferson DC, Watkins MM, Webb FH (1997) Precise point positioning for the efficient and robust analysis of GPS data from large networks. J Geophys Res 102:5005–5017